Seedless and Templateless Synthesis of Rectangular Palladium Nanoparticles

Yuan Sun,[†] Lihua Zhang,[‡] Hongwen Zhou,[§] Yimei Zhu,[‡] Eli Sutter,[‡] Yuan Ji,[†] Miriam H. Rafailovich,*[,†] and Jonathan C. Sokolov[†]

Department of Materials Science and Engineering, SUNY Stony Brook, New York 11794, Center for Functional Nanomaterials, Brookhaven National Laboratory, Upton, New York 11973-5000, and Department of Chemistry, SUNY Stony Brook, New York 11794

Received September 27, 2006. Revised Manuscript Received November 9, 2006

Highly crystalline rectangular palladium nanoparticles have been successfully synthesized via the reduction of K_2PdCl_4 by ascorbic acid in the presence of a surfactant, cetyltrimethylammonium bromide, under room temperature and trisodium citrate is a key factor for high yield of nanocubes and nanorods. The average length and aspect ratio of the nanorods can be tuned by varying the concentration of trisodium citrate. These rectangular nanoparticles were stable for months as colloids. However, after exposure to air for about 100 days, the dry nanoparticles on TEM grids were oxidized to form shells of 1.6−3.8 nm thick covering the nanoparticle surfaces.

Introduction

The optical, magnetic, catalytic, and electronic properties of nanoparticles are affected not only by the size but also by the shape.[1−4] Recently, much attention has been paid to the development of novel synthetic methodologies for making nanocrystals with specific shapes such as rods or cubes. For example, CdSe and cobalt nanorods were made by injecting an organometallic precursor into a hot surfactant mixture under inert atmosphere.[5] Gold, silver, and other metallic nanorods have been produced using seeding growth method,[6] nonseeding method,[7] electrochemical[8] or photochemical[9] reduction method in aqueous micellar templates, and rigid templates such as porous alumina[10−12] or porous polycarbonate membranes.[13] Metal nitride and carbide nanorods were synthesized through carbon nanotube-confined reactions.[14] Recently, Xia and colleagues made palladium nanocubes[15a] and triangular and hexagonal nanoplates[15b] via reduction of Na_2PdCl_4 by ethylene glycol in the presence of poly(vinyl pyrrolidone) as well as palladium nanoboxes and nanocages[15c] by a corrosive pitting and etching process. Tian and colleagues employed anodic aluminum oxide templates to fabricate palladium nanowire and nanorod arrays on substrates.[16] Eaton and colleagues discovered that RNA sequences could mediate the growth of hexagonal plates and cubic particles of palladium.[17] However, very little work has been reported on the simple, one-pot, colloidal synthesis of palladium nanocubes or nanorods at ambient temperature, especially without using seeds or rigid templates. In this paper, we report on the use of ascorbic acid, in the presence of trisodium citrate and a surfactant, cetyltrimethylammonium bromide (CTAB), to prepare rectangular Pd nanoparticles, including nanocubes and nanorods. Our procedure is conducted under room temperature and requires no seed-mediated growth or nanoporous rigid template so that it is easier and more practical for large-scale synthesis.

* To whom correspondence should be addressed. E-mail: mrafailovich@notes.cc.sunysb.edu.
[†] Department of Materials Science and Engineering, SUNY Stony Brook.
[‡] Brookhaven National Laboratory.
[§] Department of Chemistry, SUNY Stony Brook.

(1) Creighton, J. A.; Eadon, D. G. *J. Chem. Soc., Faraday Trans.* **1991**, *87*, 3881.
(2) Link, S.; El-Sayed, M. A. *J. Phys. Chem. B* **1999**, *103*, 8410.
(3) Wang, Z. L. *J. Phys. Chem. B* **2000**, *104*, 1153.
(4) Cao, Y. W.; Jin, R.; Mirkin, C. A. *J. Am. Chem. Soc.* **2001**, *123*, 7961.
(5) (a) Peng, X.; Manna, L.; Yang, W.; Wickham, J.; Scher, E.; Kadavanich, A.; Alivisatos, A. P. *Nature* **2000**, *404*, 59. (b) Puntes, V. F.; Krishnan, K. M.; Alivisatos, A. P. *Science* **2001**, *291*, 2115.
(6) (a) Jana, N. R.; Gearheart, L.; Murphy, C. J. *J. Phys. Chem. B* **2001**, *105*, 4065. (b) Gole, A.; Murphy, C. J. *Chem. Mater.* **2004**, *16*, 3633. (c) Jana, N. R.; Gearheart, L.; Murphy, C. J. *Chem. Commun.* **2001**, *7*, 617. (d) Jane, N. R.; Gearheart, L.; Murphy, C. J. *Adv. Mater.* **2001**, *13*, 1389. (e) Gao, J.; Bender, C. M.; Murphy, C. J. *Langmuir* **2003**, *19*, 9065. (f) Sau, T. K.; Murphy, C. J. *J. Am. Chem. Soc.* **2004**, *126*, 8648. (g) Johnson, C. J.; Dujardin, E.; Davis, S. A.; Murphy, C. J.; Mann, S. *J. Mater. Chem.* **2002**, *12*, 1765.
(7) Jana, N. R. *Small* **2005**, *1*, 875.
(8) (a) Yu, Y.-Y.; Chang, S.-S.; Lee, C.-L.; Wang, C. R. C. *J. Phys. Chem. B* **1997**, *101*, 6661. (b) Chang, S.-S.; Shih, C.-W.; Chen, C.-D.; Lai, W.-C.; Wang, C. R. C. *Langmuir* **1999**, *15*, 701.
(9) Kim, F.; Song, J. H.; Yang, P. *J. Am. Chem. Soc.* **2002**, *124*, 14316.
(10) Martin, B. R.; Dermody, D. J.; Reiss, B. D.; Fang, M.; Lyon, L. A.; Natan, M. J.; Mallouk, T. E. *Adv. Mater.* **1999**, *11*, 1021.
(11) Martin, C. R. *Chem. Mater.* **1996**, *8*, 1739.
(12) van der Zande, B. M. I.; Böhmer, M. R.; Fokkink, L. G. J.; Schönenberger, C. *J. Phys. Chem. B* **1997**, *101*, 852.
(13) Schönenberger, C.; van der Zande, B. M. I.; Fokkink, L. G. J.; Henny, M.; Schmid, C.; Krüger, M.; Bachtold, A.; Huber, R.; Birk, H.; Staufer, U. *J. Phys. Chem. B* **1997**, *101*, 5497.
(14) (a) Wong, E. W.; Maynor, B. W.; Burns, L. D.; Lieber, C. M. *Chem. Mater.* **1996**, *8*, 2041. (b) Han, W.; Fan, S.; Li, Q.; Hu, Y. *Science* **1997**, *277*, 1287.
(15) (a) Xiong, Y.; Chen, J.; Wiley, B.; Xia, Y.; Yin, Y.; Li, Z.-Y. *Nano Lett.* **2005**, *5*, 1237. (b) Xiong, Y.; McLellan, J. M.; Chen, J.; Yin, Y.; Li, Z.-Y.; Xia, Y. *J. Am. Chem. Soc.* **2005**, *127*, 17118. (c) Xiong, Y.; Wiley, B.; Chen, J.; Li, Z.-Y.; Yin, Y.; Xia, Y. *Angew. Chem., Int. Ed.* **2005**, *44*, 7913.
(16) (a) Yao, J.-L.; Tang, J.; Wu, D.-Y.; Sun, D.-M.; Xue, K.-H.; Ren, B.; Mao, B.-W.; Tian, Z.-Q. *Surf. Sci.* **2002**, *514*, 108. (b) Tian, Z.-Q.; Ren, B.; Wu, D.-Y. *J. Phys. Chem. B* **2002**, *106*, 9463.
(17) (a) Gugliotti, L. A.; Feldheim, D. L.; Eaton, B. E. *Science* **2004**, *304*, 850. (b) Gugliotti, L. A.; Feldheim, D. L.; Eaton, B. E. *J. Am. Chem. Soc.* **2005**, *127*, 17814.

10.1021/cm0623209 CCC: $37.00
Published on Web 03/23/2007

Nanoparticles beyond a certain size have a tendency to flocculate since their van der Waals interactions could overwhelm the steric stabilization provided by surfactants.[18] Therefore, large nanoparticles are relatively harder to form compared to small ones. Our simple procedure can easily make large rectangular Pd nanoparticles (>20 nm) which are stable for months as colloids. Moreover, since palladium catalyst is the most used among precious metal catalysts for diversified purposes, Pd nanoparticles with well-defined facets might be good models in clarifying the catalytic properties of different crystal facets.

CTAB has been widely used in the synthesis of gold and silver nanorods by electrochemical reduction[8] and chemical reduction[6,7] where nanorod growth may take place as a result of the preferential binding of CTAB to the {100} crystal facets.[6g] A bilayer of CTAB was found to form around the gold nanorods in which the cationic head groups of the inner layer was bound to the gold surface.[19] In dilute aqueous solution (>1 mM) containing no added electrolyte, the surfactant CTAB forms spherical micelles,[20] which transforms to cylindrical micelles at higher concentrations (>20 mM), rodlike micelles in the presence of organic additives,[21] and wormlike structures in the presence of salicylic acid.[22] Therefore, some researchers claimed that CTAB acted as micelle templates in the formation of gold nanorods[7] and gold−silver nanowires.[23] In our synthesis, since the concentration of CTAB (8 mM) is not high enough to form cylindrical micelles, we believe that CTAB molecules are more likely to act as a surface passivating agent which dictates the growth of rectangular Pd nanoparticles.

However, we found that CTAB alone could not result in the efficient formation of rectangular Pd nanoparticles. The presence of trisodium citrate in the reaction was necessary for the generation of large amounts of rectangular Pd nanoparticles. We studied the concentration effect of trisodium citrate on the formation of rectangular Pd nanoparticles and characterized these nanoparticles using transmission electron microscopy (TEM), scanning electron microscopy (SEM), and UV−vis spectroscopy.

Experimental Section

Synthesis of Palladium Nanoparticles. K_2PdCl_4 was reduced by ascorbic acid in the presence of CTAB and trisodium citrate. A "stock" solution was made by mixing aqueous solutions of K_2PdCl_4 and CTAB. Upon mixing, the solution changed color from light yellow to orange. A similar phenomenon had been reported by Murphy and colleagues[6e] when they mixed CTAB solution with $HAuCl_4$ solution and then made Au nanorods later. Esumi and colleagues[24] claimed that $AuCl_4^-$ formed an ion pair with CTA^+ in their synthetic procedures of making fiber-like Au particles. Therefore, we believed that the color changing upon mixing might indicate the formation of the $CTA^+[PdCl_4]^{2-}$ complex ions. The stock solution consisted of 2.5×10^{-4} M K_2PdCl_4 and 8×10^{-3} M CTAB in water. Six clean centrifuge tubes containing different amounts of trisodium citrate dihydrate were labeled A, B, C, D, E, and F. Into each tube we placed 45 mL of the stock solution, which dissolved trisodium citrate completely in a few seconds. The concentrations of trisodium citrate were 0, 0.2, 0.4, 0.6, 0.8, and 1.0×10^{-3} M in tubes A, B, C, D, E, and F, respectively. Then 250 μL of 0.1 M freshly prepared ascorbic acid aqueous solution was added to each of the six tubes. Within 15 min, the color of the mixture changed from orange to dark brown. Four days later the mixture in each of the six tubes was centrifuged at 5000 rpm for 20 min to remove most of the surfactant, and then a small amount of fresh water was added to get homogeneous black suspensions, which were stable over a few months. The suspensions were labeled as samples A, B, C, D, E, and F, respectively.

Transmission Electron Microscopy. TEM and electron diffraction analysis was performed on a Philips CM12 TEM operating at 100 keV. High-resolution TEM (HRTEM) analysis was achieved on JEOL 3000F operating at 300 keV. A droplet of dilute solution of each sample was evaporated onto the carbon-coated side of a 400-mesh copper TEM grid.

Scanning Electron Microscopy. SEM measurements were performed on LEO-1550. The dilute solutions of the samples were dried on silicon wafers, which were treated with a $H_2SO_4/H_2O_2/H_2O$ mixture under boiling temperature and rinsed with deionized water.

UV−Visible Spectroscopy. UV−vis measurements of dilute solutions of the samples were performed on Varian Cary 100 Bio UV−Visible spectrophotometer.

Results and Discussion

Concentration Effect of Trisodium Citrate. To study the effect of trisodium citrate, we synthesized the particles under six different concentrations, 0 M (sample A), 0.2 mM (B), 0.4 mM (C), 0.6 mM (D), 0.8 mM (E), and 1.0 mM (F), while we kept the concentrations of all other chemicals fixed. The concentration effect of trisodium citrate can be seen clearly in the TEM images of sample A−F, as given in Figure 1. The absence of trisodium citrate resulted in a majority of almost spherical nanoparticles which showed some facets (sample A). However, the presence of trisodium citrate was a trigger for the formation of rectangular particles, including nanocubes and nanorods (samples B−F). Based on at least four TEM measurements per sample, which represented 500−900 particles, the percentages of nanocubes and nanorods in each sample were estimated and plotted as histograms in Figure 2. From the figure we find that[25] the percentage of nanorods ranges from 63% to 81% but no obvious relation to the concentration of trisodium citrate can be observed. However, the mean length and the average aspect ratio of the nanorods increased as the trisodium citrate concentration increased from 0.2 to 1.0 mM, while the edge length of the nanocubes and the width of the nanorods did not change too much, as shown in Table 1. Another phenomenon we observed was the well-ordered self-as-

(18) Israelachvili, J. N. *Intermolecular and Surface Forces*, 2nd ed.; Academic Press: New York, 1992; Chapter 10.
(19) Nikoobakht, B.; El-Sayed, M. A. *Langmuir* **2001**, *17*, 6368.
(20) Kalyanasundaram, K. *Photochemistry in Microheterogeneous Systems*; Acadamic Press: New York, 1987.
(21) Lindemuth, P. M.; Bertrand, G. L. *J. Phys. Chem.* **1993**, *97*, 7769.
(22) Lin, Z.; Cai, J. J.; Scriven, L. E.; Davis, H. T. *J. Phys. Chem.* **1994**, *98*, 5984.
(23) Krichevski, O.; Tirosh, E.; Markovich, G. *Langmuir* **2006**, *22*, 867.
(24) Kameo, A.; Suzuki, A.; Torigoe, K.; Esumi, K. *J. Colloid Interface Sci.* **2001**, *241*, 289.

(25) It should be noted that each image shown in Figure 1 is only a small portion of one of the images used to obtain these percentages. The images were chosen for clarity and hence were not necessarily the illustrations of the averaged results.

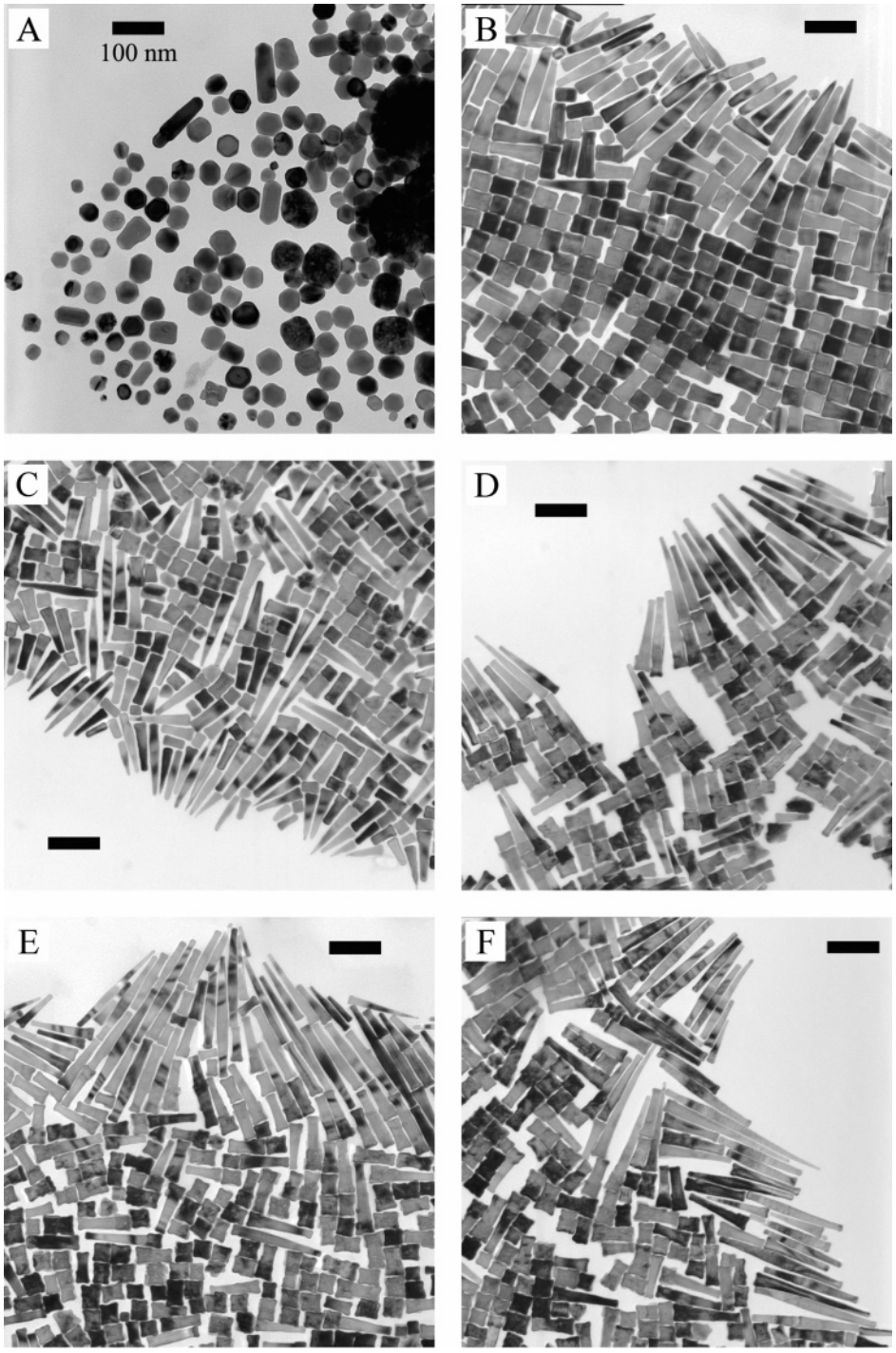

Figure 1. TEM images of Pd nanoparticles made from six different concentrations of trisodium citrate: (A) 0; (B) 0.2 mM; (C) 0.4 mM; (D) 0.6 mM; (E) 0.8 mM; and (F) 1.0 mM. Scale bar represents 100 nm.

sembled monolayer of the rectangular nanoparticles which showed some degree of size and shape segregations, especially in sample B.

Except for the monolayer, the particles also piled up and formed multilayers when they were dried from solutions on solid substrates. This was illustrated in Figure 3b, an SEM image taken on a silicon wafer tilted by 45°. The thickness of the particles was estimated to be 30 nm from the fairly large ensemble present which appeared fairly uniform. An atomic force microscopy (AFM) measurement on a particle cluster (see Supporting Information) showed that the height or thickness of the particles was the same as that estimated from the SEM image after tilting (Figure 3b). We therefore conclude that the cross sections of both nanocubes and nanorods are rectangular.

HRTEM images and electron diffraction patterns revealed that each rectangular Pd nanoparticle was a perfect single crystal with a face-centered cubic (fcc) structure. Figures 4a and 4b are HRTEM images of a nanocube and a nanorod, respectively, which show that both are oriented with the ⟨100⟩ direction, parallel to the incident beam. We note that the nanocubes have strong (100) faceting, while growth directions of the nanorods are along the major axes (⟨100⟩) of the crystals. High-resolution imaging and diffraction analyses

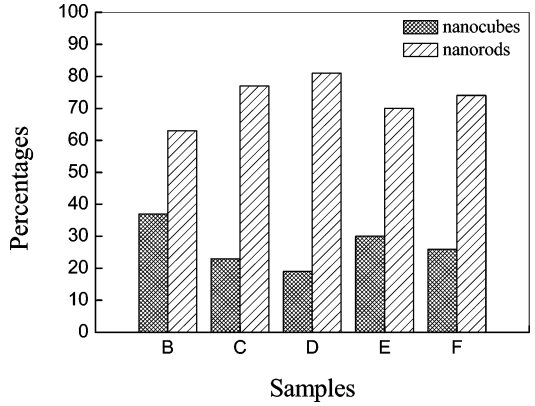

Figure 2. Estimation of the percentages of nanocubes and nanorods in samples B−F based on TEM images.

Table 1. Size Information of the Rectangular Particles Measured from TEM Pictures[a]

sample	edge length of the nanocubes (nm)	width of the nanorods (nm)	length of the nanorods (nm)	aspect ratio of the nanorods
B	31.8 ± 0.1	27.2 ± 0.1	64.2 ± 1.0	2.48 ± 0.04
C	26.7 ± 0.2	20.1 ± 0.1	65.3 ± 1.0	3.41 ± 0.06
D	27.4 ± 0.3	21.0 ± 0.1	72.3 ± 1.3	3.68 ± 0.08
E	27.8 ± 0.2	21.7 ± 0.1	80.3 ± 1.3	4.00 ± 0.08
F	29.4 ± 0.2	21.6 ± 0.1	78.9 ± 1.1	3.94 ± 0.06

[a] For each distribution, the uncertainty is the standard deviation of the mean.

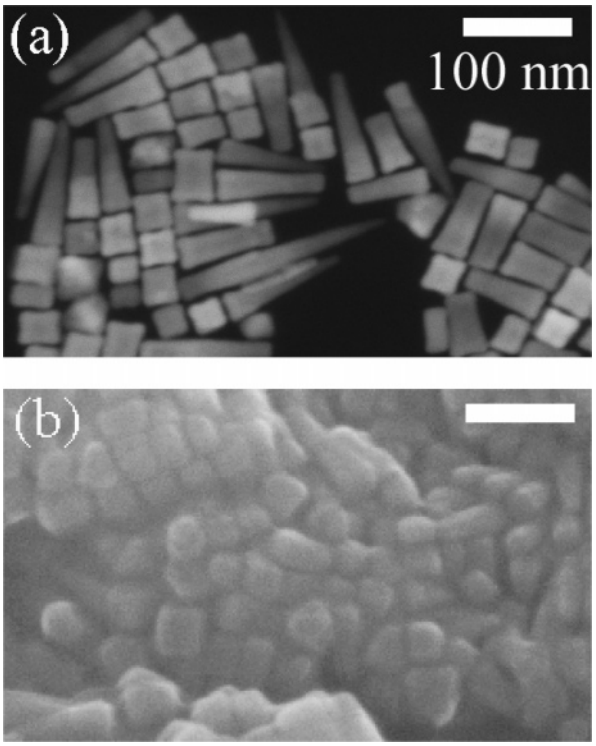

Figure 3. SEM images of sample B dried on a silicon wafer (a) before and (b) after being tilted by 45°, confirming the rectangular cross sections and indicating the thickness of the Pd particles was about 30 nm. Scale bar represents 100 nm.

of single nanoparticles (Figure 4c) suggest a lattice parameter a_0 of 3.84 Å, while the diffraction ring pattern (Figure 4d), which averages over a few dozen particles, gave a lattice parameter of 3.79 Å. Both values are slightly shorter than the bulk value of Pd (3.89 Å[26]).

(26) JCPDS-International Centre for Diffraction Data.

A more careful observation of Figures 1B−1F reveals that the corners of the rectangular Pd nanoparticles are not sharp. This can be seen even more clearly in the enlarged corner shown in Figure 4a. In many cases, the corners are even more protrusive. It is possible that the geometry of a 90° corner, where the (100) and (010) planes meet, are not energetically favorable for crystal growth. Therefore, a more accessible growth direction is chosen which results in a rounded corner. Since this direction is energetically favored, crystal overgrowth can occur and produce the protrusions. We think that this favored growth is probably along [111] directions, which has been found in the overgrowth of Au nanorods.[27]

It is well-known that spherical gold nanoparticles exhibit a single absorption band in the UV−vis range attributed to the surface plasma resonance. This single absorption band splits into two bands, the longitudinal resonance and the transverse resonance, when the eccentricity of the gold nanoparticles increases.[6a,e,b,8a] UV−vis measurements were conducted on our rectangular palladium nanoparticles. Figure 5 is a typical UV−vis absorption spectrum measured from diluted sample B, showing continuous absorption across the range. This is in good agreement with the theoretic calculations[1] based on Mie theory which predicted that colloidal palladium exhibited only rather broad absorption continua which extended throughout the visible-near-ultraviolet range.

In our experiments, a large amount of rectangular Pd nanoparticles were found to form in 20 h. However, to allow the reaction to complete thoroughly, we waited 4 days to conduct further actions. TEM results showed that the rectangular Pd nanoparticles did not grow in width or length after 20 h of reaction.

Growth Mechanism. As mentioned in the Introduction, the growth mechanism of nanorods in the presence of CTAB has not been clearly understood. Some researchers believed that it was due to the preferential binding of CTAB to certain crystal facets and a "zipping" mechanism was proposed;[6e] others thought the crystal growth was confined in the cylindrical micelles of CTAB.[7,23] In our case, since the CTAB concentration is not high enough to form cylindrical micelles, we believe that CTAB molecules are more likely to act as surface passivating agent which directs the growth of rectangular Pd nanoparticles. In the synthesis of nanorods, small-sized nanoparticles were widely used as seeds where further crystal growth occurred. In our seedless one-step synthesis, the nucleation could be initiated by either trisodium citrate or ascorbic acid. It is well-known that $[PdCl_4]^{2-}$ ions can be reduced by trisodium citrate to generate Pd nanoparticles in boiling aqueous solution[28,29] but not under room temperature. Our experiments (see Supporting Information) showed that under room temperature $[PdCl_4]^{2-}$ ions could be reduced by ascorbic acid to form 3-nm nanospheres and adding trisodium citrate had no effect on the formation of the nanospheres and their sizes (CTAB was not used in the synthesis). Therefore, we believed that, in our nonseeding

(27) Song, J. H.; Kim, F.; Kim, D.; Yang, P. *Chem. Eur. J.* **2005**, *11*, 910.
(28) Turkevich, J.; Kim, G. *Science* **1970**, *169*, 873.
(29) Schmid, G.; West, H.; Mehles, H.; Lehnert, A. *Inorg. Chem.* **1997**, *36*, 891.

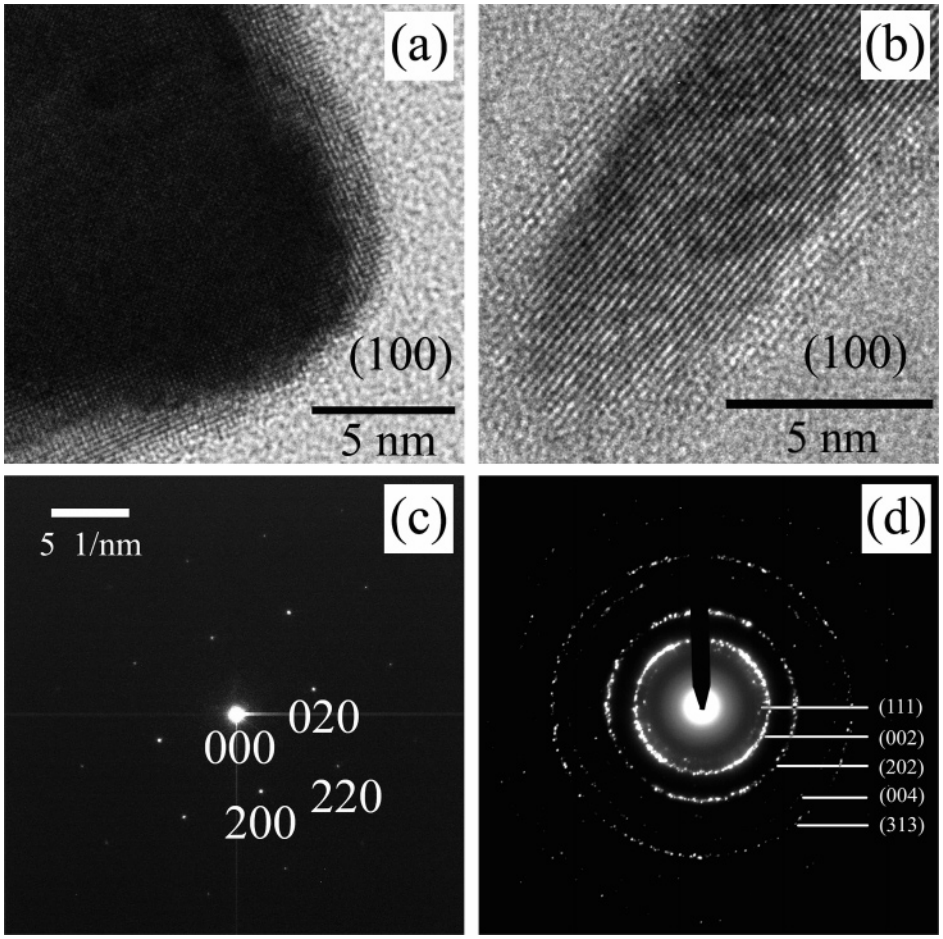

Figure 4. HRTEM images of (a) a corner of a Pd nanocube and (b) an end of a Pd nanorod oriented with the ⟨100⟩ direction parallel to the incident beam; (c) the (100) zone electron diffraction pattern of a single Pd particle; (d) electron diffraction ring pattern from an area covering several dozens of Pd particles (both patterns can be indexed as fcc).

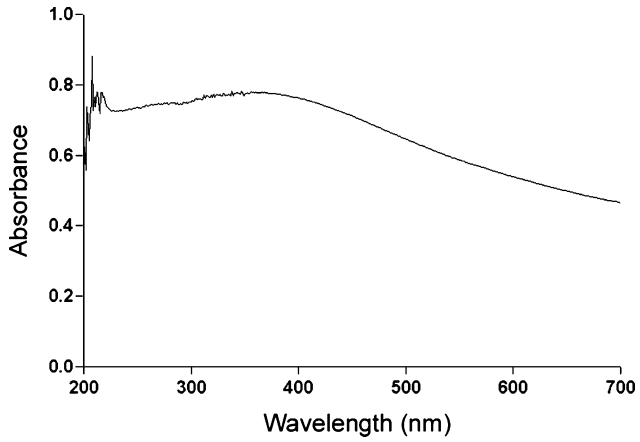

Figure 5. UV−vis absorption spectrum of sample B shows continuous absorption across the range.

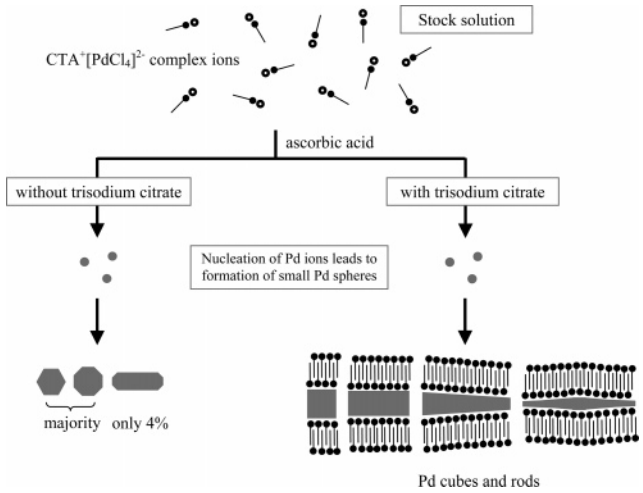

Figure 6. Proposed growth mechanism showing nucleation and growth of Pd nanocubes and nanorods. The open circles represent $[PdCl_4]^{2-}$ ions; the black dots with the short straight lines represent cetyltrimethylammonium ions, where the black dots are the hydrophilic head groups and the short straight lines are the hydrophobic tails.

synthesis of the rectangular Pd nanoparticles conducted under room temperature, ascorbic acid acted as the only reducing agent to initiate the nucleation and CTAB acted as a directing surfactant to help the growth of the nanoparticles.

A possible growth mechanism was proposed as shown in Figure 6. $CTA^+[PdCl_4]^{2-}$ complex ions form upon the mixing of K_2PdCl_4 and CTAB. Then ascorbic acid reduces the complex ions to generate small Pd spheres. As we mentioned before, the presence of trisodium citrate was a trigger for the formation of rectangular particles. A possible explanation is that, under the assistance of trisodium citrate, the preferential binding of CTAB to the (100) crystal facet is initiated and assists nanocube and nanorod formation as more Pd ions are reduced. Increasing the concentration of trisodium citrate might enhance the binding of CTAB to the particle surface; therefore, longer nanorods forms. Without trisodium citrate, the small Pd spheres grow without preferential directs.

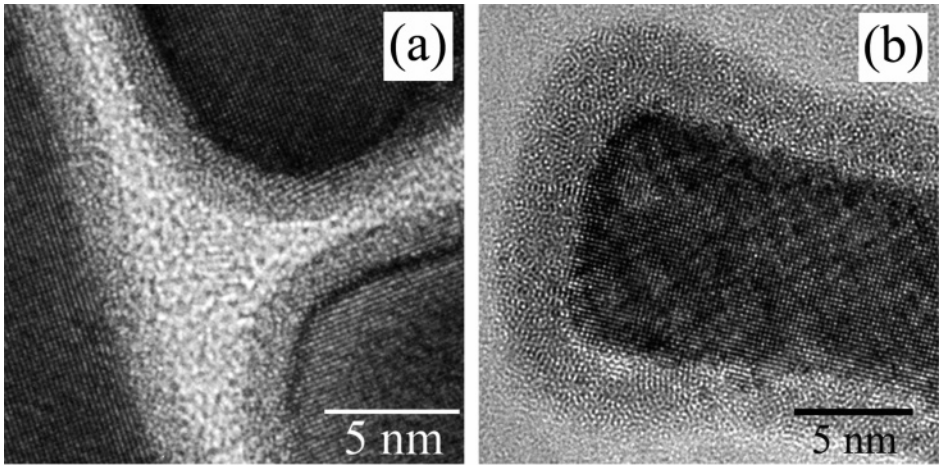

Figure 7. (a) HRTEM images of sections of three oxidized Pd particles; (b) magnified image of an oxidized Pd nanorod.

Another possibility is that varying the concentrations of trisodium citrate may induce electrolyte effect on the system, which favors the generation of rectangular nanoparticles. In addition, the co-adsorption of trisodium citrate and CTAB to both Pd ionic precursor and nanoparticle facets could also be responsible for directing the nanoparticle growth and therefore affecting the morphology of the nanoparticles, due to the intrinsic coordinating property of trisodium citrate. Although both CTAB and trisodium citrate have coordination abilities and are widely used as capping agents, neither of them could individually mediate the formation of rectangular Pd nanoparticles in our case; they have to work in the presence of each other. More research needs to be done to understand the mechanism and kinetics of the shape control, such as the roles of the concentrations of CTAB, Pd salt, ascorbic acid, the temperature, etc. It is interesting to note that the reaction kinetics will change at higher temperatures, and in particular the sodium citrate may now compete as a reductant. Since the growth kinetics and reduction rate greatly affect the shape of the nanoparticles, interesting new structures may be formed. This is a topic under current investigation and will be published at a later date.

Oxidation of the Nanoparticles. After being exposed to air for about 100 days, an amorphous shell with thickness of 1.6−3.8 nm is found under TEM, which is believed to be palladium oxide. The oxide shell was independent of particle size, length, or aspect ratio. Xia and colleagues[15a] also reported that an oxide layer would form on Pd nanocubes with sizes of 25 and 50 nm. Figure 7a is a top view of three oxidized particles where shell can be seen around all the edges. In this case the corners do not protrude and the shell appears to have a uniform thickness of 1.6 nm. In Figure 7b we show the shell around a nanorod particle with protruding corners. Here we see that the shell is significantly thicker (2.4−3.8 nm) around the protrusion. This indicates that the protruding configuration may be more prone to oxidation.

Our unresolved issues are the finer control of the uniformity of the nanoparticle formation and the separation of nanocubes from nanorods. These problems might be solved by decreasing the rate of crystallization via weaker reducing agent and increasing the concentration of CTAB to enhance the shape control. Besides, a more detailed study on the growth mechanism is needed to understand exactly how trisodium citrate assists the surfactant CTAB to direct the anisotropic nanoparticle growth.

Conclusion

We have developed a simple synthetic procedure to make rectangular Pd nanoparticles without using seeds or rigid templates. Under the assistance of trisodium citrate, the preferential binding of CTAB to the (100) crystal facet may lead to the formation of rectangular Pd nanoparticles, including nanocubes and nanorods. The average length and aspect ratio of the nanorods can be tuned by the concentration of trisodium citrate. HRTEM images and diffraction patterns indicate that the particles are perfect single crystals of ⟨100⟩ orientation. Oxidation of the dried particles occurs after being exposed to air for 100 days. The oxide is manifested as a shell around the exterior of the particles, approximately 1.6−3.8 nm thick. The shell thickens around protruding corners, indicating that the easy direction of crystallization may be more sensitive to oxidation. Future work will be conducted to understand the growth mechanism and kinetics of the rectangular Pd nanoparticles and to find the optimum synthetic conditions to improve shape control.

Acknowledgment. Supported by NSF-MRSEC program. Research carried out in part at the Center for Functional Nanomaterials, Brookhaven National Laboratory, which is supported by the U.S. Department of Energy, Division of Materials Sciences, and Division of Chemical Sciences, under Contract No. DE-AC02-98CH10886. The authors gratefully acknowledge the assistance of Dr. James Quinn for SEM measurements, Dr. Yantian Wang for AFM measurements, and Dr. Jie Bai for HRTEM analysis.

Supporting Information Available: TEM pictures of the 3-nm Pd nanospheres synthesized via the reduction of K_2PdCl_4 by ascorbic acid. AFM measurement on a particle cluster showing that the height or thickness of the particles appeared the same as that estimated from the SEM image after tilting. This material is available free of charge via the Internet at http://pubs.acs.org.

CM0623209